Original Article

Characterization and assessment of the potential use of charcoal ash in cementitious composites

*Elias Rocha Gonçalves Júnior 1**
Esther Tavares 1
Afonso Rangel Garcez de Azevedo 2
Markssuel Teixeira Marvila 3

Abstract

This study evaluated the use of charcoal ash (CA-ash) as a partial replacement for Portland cement in mortars. X-ray fluorescence revealed high CaO (≈69%) and K2O (≈11%) contents, while X-ray diffraction identified crystalline phases of quartz and sylvite, confirming the non-pozzolanic nature of the ash. Laser granulometry indicated a median particle size of approximately 19 µm. Isothermal calorimetry showed a reduction in heat flow and cumulative heat release with increasing CA-ash content, mainly due to clinker dilution. In the fresh state, the incorporation of 5% and 10% CA-ash reduced the consistency index from 264 mm in the reference mixture to approximately 230 mm and 215 mm, respectively. The mixture containing 5% CA-ash exhibited the highest compressive strength, increasing from about 10 MPa in the reference mortar to approximately 14 MPa at 7 days. Water absorption (≈10.6%), open porosity (≈20%), and apparent density (1.83-1.89 g/cm3) showed only minor variations among mixtures. Statistical analysis (ANOVA) indicated that mixture composition significantly affected compressive strength and apparent density, whereas water absorption and open porosity were not statistically influenced. Overall, CA-ash behaves predominantly as an inert filler that improves early mechanical performance while maintaining matrix compactness.

Keywords: Charcoal ash; Supplementary cementitious material; Mortar.

1 Introduction

The civil construction industry is one of the sectors that consumes the largest amounts of natural resources and energy [1]. Globally, the construction sector accounts for approximately 30-40% of total material extraction and energy consumption, reflecting its large-scale demand for raw materials and infrastructure development [2,3]. This high demand, combined with the carbon dioxide (CO2) emissions associated with Portland cement production, has driven the development of strategies aimed at sustainability and the reduction of environmental impacts [4]. Cement production alone is responsible for around 7-8% of global anthropogenic CO2 emissions, mainly due to clinker calcination and fuel combustion processes [4]. In this context, the reuse of solid waste has emerged as a promising alternative for the formulation of more efficient and environmentally responsible cementitious materials [5].

Among the available residues, ashes derived from biomass combustion have gained attention due to its wide availability in both urban and rural contexts. Biomass represents a significant fraction of energy consumption worldwide, and its combustion generates substantial quantities of ash residues that require appropriate management and environmentally sound disposal routes [6]. Charcoal production and combustion processes are also associated with the emission of greenhouse gases, including CO2, CO and CH4, with life cycle assessments reporting emissions of approximately ~2.4 t CO2-eq/t charcoal depending on process efficiency and production conditions [7], contributing to global warming, particularly under uncontrolled conditions such as domestic and commercial cooking. Charcoal ash, generated in households and commercial establishments that use charcoal for food preparation [8,9], remains largely unexplored as a material of interest for civil engineering applications.

Despite its significant volume, given that Brazil leads global charcoal production with approximately 6.6 million tonnes per year [10], and its often-inadequate disposal, this residue still lacks systematic studies investigating its feasibility as an alternative cementitious material. Biomass combustion produces solid residues such as ash, typically ranging from 0.5% to 7% of the initial mass [11], along with unburned carbon fractions, and the incorporation of such

[1]*Laboratório de Materiais Avançados, Universidade Estadual do Norte do Rio de Janeiro Darcy Ribeiro – UENF, Campos dos Goytacazes, RJ, Brasil.*
[2]*Laboratório de Engenharia Civil, Universidade Estadual do Norte do Rio de Janeiro Darcy Ribeiro – UENF, Campos dos Goytacazes, RJ, Brasil.*
[3]*Departamento de Engenharia Civil, Universidade Federal de Viçosa – UFV, Rio Paranaíba, MG, Brasil.*

**Corresponding author: eliasrgjunior1@gmail.com*
E-mails: esthertavares.e@gmail.com; afonso@uenf.br; markssuel.marvila@ufv.br

residues as partial cement replacements has been investigated as a strategy to reduce overall CO2 emissions by decreasing clinker consumption, particularly in comparison with highly pozzolanic ashes such as rice husk ash and sugarcane bagasse ash [12,13]. However, limited information is available regarding the emission balance and performance of charcoal ash derived from food preparation, especially in mortar systems, highlighting a gap in the literature concerning both its environmental implications and its behavior in cement-based materials.

The behavior of biomass ashes in cementitious composites depends on several factors, such as combustion conditions, chemical composition, particle size distribution, and the presence of soluble impurities [14]. These characteristics directly influence the material's properties, potentially affecting cement hydration, microstructure formation, and the physical and mechanical performance of the composite [6]. Depending on its mineralogical and granulometric characteristics, charcoal ash may act either as a supplementary cementitious material with pozzolanic potential or predominantly as a filler, contributing mainly through physical effects [15]. Nevertheless, there is a scarcity of studies that comprehensively assess how charcoal ash influences the properties of pastes and mortars, particularly regarding hydration development and the resulting hardened-state performance.

Therefore, this paper aims to evaluate the potential application of charcoal ash in cementitious composites and to investigate how its incorporation affects the physical, chemical, and mechanical behavior of the system. For this purpose, the ash characteristics were analyzed, the hydration process of pastes was examined through isothermal calorimetry tests, and the performance of mortars was evaluated in terms of compressive strength, water absorption, open porosity, and apparent density.

By providing a systematic evaluation of this underutilized urban residue, this research contributes technical insights into its feasibility and limitations for use in more sustainable cementitious formulations.

2 Material and methods

2.1 Raw materials

The Portland cement used in this study was CP II F-32. It was selected for its widespread use in conventional construction and its compliance with pozzolanic material testing requirements established by ABNT NBR 5752 [16] and ABNT NBR 16697 [17], which establishes a mineral addition content ranging from 11 to 25% for this type of cement. The fine aggregate was natural quartz sand sampled from the Paraíba do Sul River (Campos dos Goytacazes, RJ, Brazil), dried, and sieved according to NBR 7214 [18].

The charcoal ash (CA-ash) used as a partial replacement material was collected from a restaurant in Campos dos Goytacazes, Rio de Janeiro, Brazil. The residue originated from the combustion of charcoal used in food preparation, representing a typical sample of waste generated by popular brands in the sector. This type of ash reflects real conditions of residue generation in urban environments, particularly in food establishments where salt is commonly used directly on meats. Since the ash was collected as a waste material rather than produced under controlled laboratory conditions, combustion temperature and residence time could not be defined.

Prior to testing, the ash was dried in an oven at 60 °C for 24 hours and sieved through a 45 μm mesh to remove coarse impurities and ensure homogeneity. Distilled water was used in all mixtures to eliminate the influence of ions on the hydration process.

2.2 Ash characterization

Comprehensive physicochemical characterization of the CA-ash was performed to assess its composition, particle size, and reactivity. The chemical composition was determined by X-ray fluorescence (XRF) using an Epsilon 3X spectrometer (Malvern PANalytical), providing the main oxides relevant to cementitious performance [19].

The mineralogical composition was evaluated by X-ray diffraction (XRD) on a Shimadzu XRD 7000 diffractometer with Cu-Kα radiation (λ = 1.5406 Å), operating from 5° to 70° (2θ), with a step size of 0.02° and scan rate of 2°/min. Particle size distribution was obtained by laser diffraction granulometry using a Microtrac S3500 analyzer, from which the parameters d50, and d90 were recorder to quantify the median and upper-bound particle sizes, respectively.

The pozzolanic activity was qualitatively assessed using the Luxán conductivity method [20]. In this test, 5 g of CA-ash were added to 200 mL of saturated calcium hydroxide solution under magnetic stirring at 900 rpm. The electrical conductivity was monitored over 120 s using a conductivity meter (EC150, Oakton Instruments). This method was selected as a rapid screening procedure to evaluate the potential consumption of Ca2+ ions by reactive phases present in the ash. According to Luxán's classification, the variations between the final and initial electrical conductivity values lower than 0.40 mS/cm indicate a non-pozzolanic behavior, values raging from 0.40 to 1.20 mS/cm correspond to moderate pozzolanicity, and differences exceeding than 1.20 mS/cm denote high pozzolanic activity.

2.3 Isothermal calorimetry

The influence of CA-ash on cement hydration was investigated through isothermal calorimetry [21] performed using a Calmetrix I-CAL 2000 HPC calorimeter.

Pastes were prepared with ash replacement levels of 0% (reference), 5%, and 10% by mass, maintaining a water-to-binder ratio (w/b) of 0.50. The selected replacement levels represent low and moderate substitution ranges commonly adopted in preliminary screening studies of alternative additions, allowing evaluation of physical effects while limiting excessive clinker dilution [6].

The mixtures were homogenized for 5 min using a laboratory mortar mixer to ensure uniform dispersion before placement in the calorimeter. Heat flow (mW/g) was continuously monitored for the first 48 hours after mixing at a controlled temperature of 40 °C. The test enabled evaluation of the kinetics of heat release, including peak intensity, time to main peak, and cumulative heat evolution, providing insights into potential modifications of the hydration mechanism caused by the chemical and physical properties of the charcoal ash.

2.4 Mortar production and testing

In order to characterize the behavior of mortars produced with partial replacement of Portland cement by CA-ash, tests were carried out encompassing both the fresh and hardened states of the material. This approach allowed the evaluation of not only the initial workability of the mixtures but also their physical and mechanical performance over time [22].

Mortars were produced with 0%, 5%, and 10% replacement levels of CA-ash by mass. The mixtures followed a sand-to-binder ratio of 3:1 and a water-to-binder ratio (w/b) of 0.80. The w/b ratio was intentionally selected to ensure adequate workability and molding under standardized mechanical mixing conditions, while also allowing the observation of possible physical effects associated with ash incorporation. The mixture proportions were defined based on previous experimental studies and selected to ensure adequate particle packing.

Mixing was performed in three stages: (i) dry blending of cement and CA-ash for 2 min, carried out manually to ensure preliminary homogenization; (ii) addition of water followed by 3 min of mechanical mixing using a bench mortar mixer; and (iii) incorporation of sand and additional mechanical mixing for 2 min to ensure uniform dispersion.

For each formulation, 15 cylindrical specimens (5 × 10 cm) were molded in two layers and compacted with 20 strokes per layer. The specimens were demolded after 24 hours and cured under controlled laboratory conditions at (23 ± 2) °C, without controlled relative humidity until the testing ages. This curing condition allows moisture exchange with the environment and may influence hydration development, particularly under the relatively high water-to-binder ratio adopted in the study.

The consistency index was determined immediately after mixing in order to evaluate the flowability and workability of the fresh mortars, according to NBR 13276 [23]. The spread diameter was measured three times for each mixture, and the consistency index was calculated as the average of these values to assess potential variations in flow behavior.

The compressive strength was determined according to NBR 7215 [24], by applying a continuously increasing load until specimen failure. Tests were performed at 7 days, to monitor early strength development, and at 28 days, to represent the characteristic mechanical performance of the mortars. For each age and formulation, five specimens (n = 5) were tested, and results are reported as mean ± standard deviation. The specimens and the test setup used for compressive strength evaluation are shown in Figure 1.

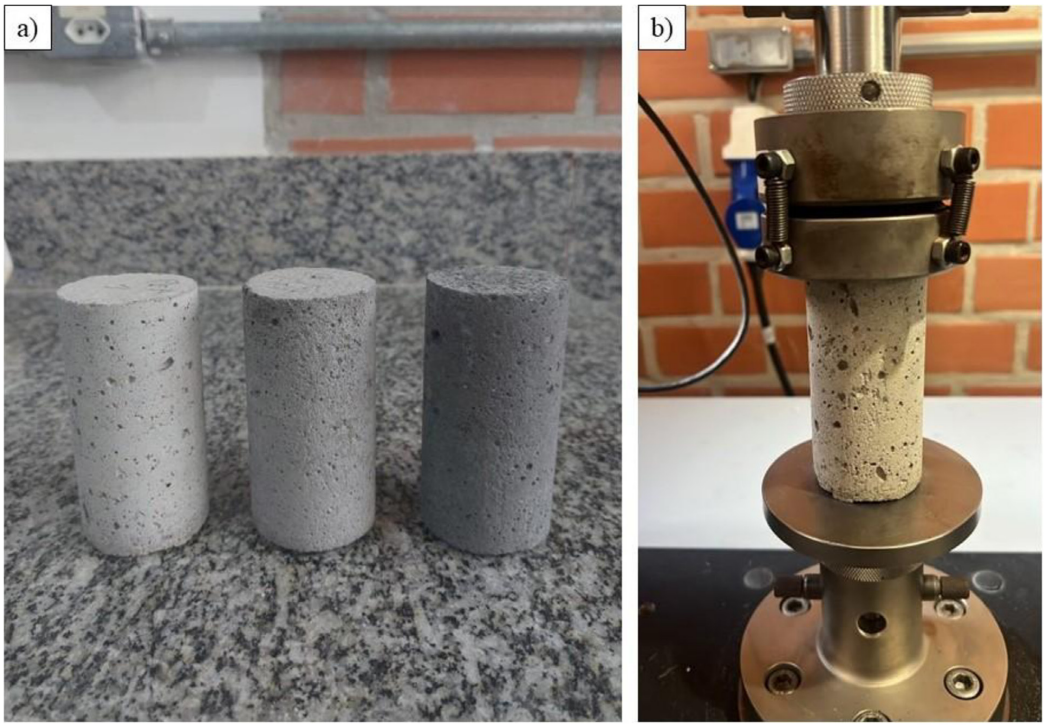

Figure 1. (a) Cylindrical mortar specimens after curing; (b) Compression test setup.

Water absorption and open porosity index tests were conducted following an adapted procedure based on ABNT NBR 9778 [25]. Initially, each specimen's mass was recorded after oven drying at 60 °C for 24 hours. The samples were then immersed in distilled water for another 24 hours to ensure complete saturation, and their saturated and submerged masses were subsequently measured. These measurements provided additional insights into the pore structure and compactness of the mortars. After completing this process, the water absorption and open porosity index values were calculated using Equations 1 and 2:

$$WA = \left[\left(m_{sat} - m_{dry} \right) / m_{dry} \right] \times 100 \quad (1)$$

$$OPI = \left[\left(m_{sat} - m_{dry} \right) / \left(m_{sat} - m_{sub} \right) \right] \times 100 \quad (2)$$

where: WA denotes the water absorption, expressed as a percentage and obtained by relating the mass gain after saturation to the dry mass of the specimen. msat corresponds to the saturated mass, mdry to the oven-dried mass, and msub to the submerged mass measured in water. The open porosity index (OPI), also expressed as a percentage, represents the ratio between the absorbed water volume and the apparent volume of the specimen, as determined from these mass measurements.

Finally, the apparent density was calculated from the ratio between the dry mass and the geometric volume of the specimens [26]. This test was performed at 28 days and allows inferences about particle packing and internal structure, as well as aiding in the interpretation of strength and porosity results. Variations in this parameter may indicate physical effects caused by the presence of charcoal ash in the internal microstructure of the mortar [27].

The experimental results were statistically analyzed in order to verify the significance of the effects associated with CA-ash replacement. For compressive strength, a two-way analysis of variance (ANOVA) was performed considering mixture composition and curing age as independent factors. For water absorption and open porosity, a two-way ANOVA was carried out considering mixture composition and property type as independent factors. Apparent density results were evaluated by one-way ANOVA considering mixture composition as the independent factor. In all cases, the significance level adopted was $\alpha = 0.05$. This approach was used to determine whether the observed differences among mixtures were statistically significant or associated with experimental variability.

3 Results and discussion

3.1 Chemical and physical characterization of CA-ash

The chemical composition of the CA-ash determined by X-ray fluorescence (XRF) is presented in Table 1. The results reveal a predominance of calcium oxide, followed by potassium oxide, chlorine, and smaller amounts of silicon dioxide, sulfur trioxide and iron oxide.

This composition indicates that the ash is rich in alkaline and alkaline-earth oxides, typical of residues derived from the combustion of lignocellulosic biomass [28,29]. The high CaO content suggests a strongly basic character, which may increase the alkalinity of the cementitious matrix and accelerate hydration reactions. In contrast, the low SiO2 and Al2O3 contents point to limited pozzolanic potential [30], corroborating previous studies that report similar behavior for charcoal and wood ashes with crystalline structures [31].

When compared to other biomass ashes reported in the literature, such as sugarcane bagasse ash (SiO2 > 70%) [32] or rice husk ash (SiO2 > 90%) [33], the chemical profile of CA-ash is markedly different, indicating that its contribution is primarily physical (filler effect) rather than chemical (pozzolanic reactivity). However, the high calcium and potassium contents may still affect the ion balance in the pore solution and promote the formation of secondary hydrates [34].

Considering the sum of SiO2 + Al2O3 + Fe2O3 (≈ 6.50%), the ash does not meet the minimum threshold typically associated with pozzolanic materials [35], which further supports its classification as a non-reactive addition under the investigated conditions. However, the high calcium and potassium contents may still affect the ion balance in the pore solution and promote the formation of secondary hydrates [31]. Nevertheless, such effects are expected to be limited to physicochemical adjustments of the pore solution rather than true pozzolanic reactions involving calcium hydroxide consumption.

The X-ray diffraction (XRD) pattern of the CA-ash is shown in Figure 2. The diffractogram reveals the predominance of crystalline phases dominated by quartz (SiO2), identified by its high-intensity peaks, and sylvite (KCl), a potassium-derived salt commonly present in biomass residues subjected to combustion. The sharp and well-defined peaks indicate a high degree of crystallinity and a low amorphous fraction [36], consistent with the uncontrolled combustion process typically associated with charcoal production [8].

Laser diffraction analysis showed a unimodal particle size distribution with a predominant peak around 19 μm, corresponding to d50 = 18.98 μm, d10 = 7.70 μm, and d90 = 32.60 μm. This particle size range is similar to that

Table 1. Chemical composition of CA-ash

Composition (%)	CaO	K2O	Cl	SiO2	SO3	Fe2O3	MnO	SrO	Others
CA-ash	69.33	11.14	9.20	5.21	2.94	1.29	0.41	0.32	0.18

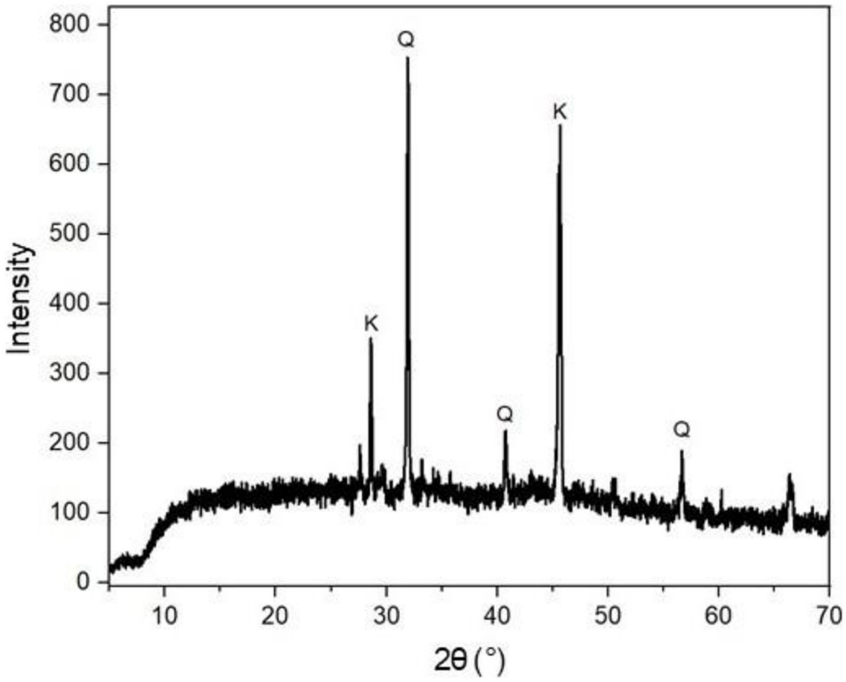

Figure 2. XRD pattern of CA-ash. Caption: Q = quartz (SiO2); K = sylvite (KCl).

of Portland cement grains (typically 10-30 μm), suggesting potential granulometric compatibility between the materials.

The particle size distribution curves of CA-ash and Portland cement are presented in Figure 3. The CA-ash exhibits a unimodal and relatively narrow distribution, characterized by a steeper cumulative slope in the intermediate particle size range. In contrast, the cement presents a broader distribution, extending toward both finer and coarser fractions.

A significant overlap between the curves is observed in the 10-30 μm range, indicating granulometric compatibility between CA-ash and cement particles. The CA-ash curve shows a slight shift toward smaller particle diameters in the intermediate region, although without a pronounced ultrafine fraction (< 5 μm) [36].

This behavior suggests that CA-ash may contribute to moderate packing adjustment by occupying interstitial spaces between cement grains. However, due to the absence of a substantial ultrafine amorphous fraction, the ash does not significantly refine the finest particle range. Therefore, any mechanical enhancement observed at low replacement levels is more plausibly attributed to physical packing effects rather than to particle size refinement or chemical reactivity.

The absence of coarse particles (> 100 μm) confirms that the sieving and drying process was effective in producing a homogeneous fine material suitable for mortar incorporation [6].

The behavior observed in the XRD analysis was confirmed by the electrical conductivity test performed according to the Luxán method [20]. The saturated calcium hydroxide solution showed an increase in conductivity from 7.06 mS/cm to 15.31 mS/cm after 120 seconds, indicating no evidence of Ca2+ ion consumption. This increase can be attributed to the release of soluble salts [37], such as chlorides and potassium compounds, resulting from biomass combustion and the presence of residual salts originating from food preparation processes.

Based on these results, the charcoal ash is classified as a non-pozzolanic material, showing no significant chemical reactivity. Its influence on the cementitious system is therefore expected to be predominantly physical, acting through particle packing and pore refinement rather than chemical interaction with calcium hydroxide [38].

Taken together, the chemical, mineralogical, granulometric, and conductivity results consistently demonstrate that CA-ash behaves as an inert mineral addition whose contribution to mortar performance is governed mainly by physical packing effects rather than hydration-related chemical reactions.

3.2 Effect of CA-ash on the hydration kinetics

The heat flow evolution of cement pastes containing 0%, 5%, and 10% CA-ash is presented in Figure 4. All mixtures exhibited the typical heat evolution profile of Portland cement hydration, characterized by two main stages: an initial peak associated with the dissolution of anhydrous compounds and a broader second peak related to the formation of hydration products such as C–S–H and ettringite. However, the reference mixture (0%) released the highest heat flow, followed by the 5% and 10% replacement mixtures.

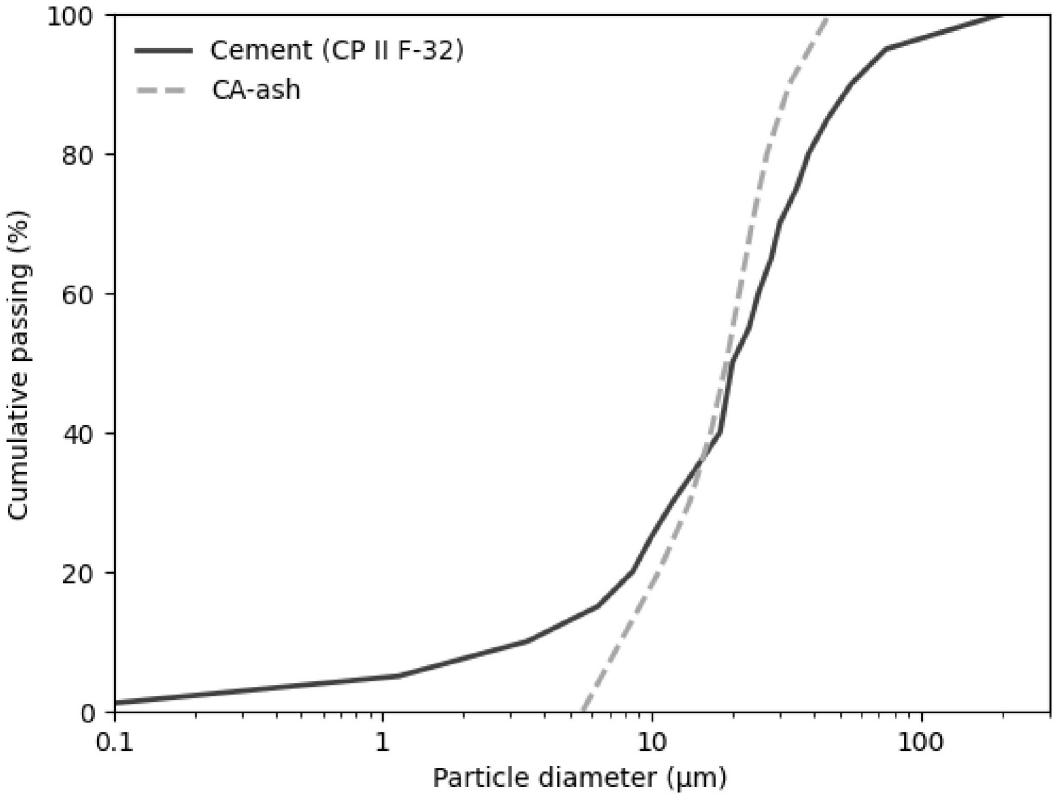

Figure 3. Particle size distribution curves of CA-ash and Portland cement (CP II F-32).

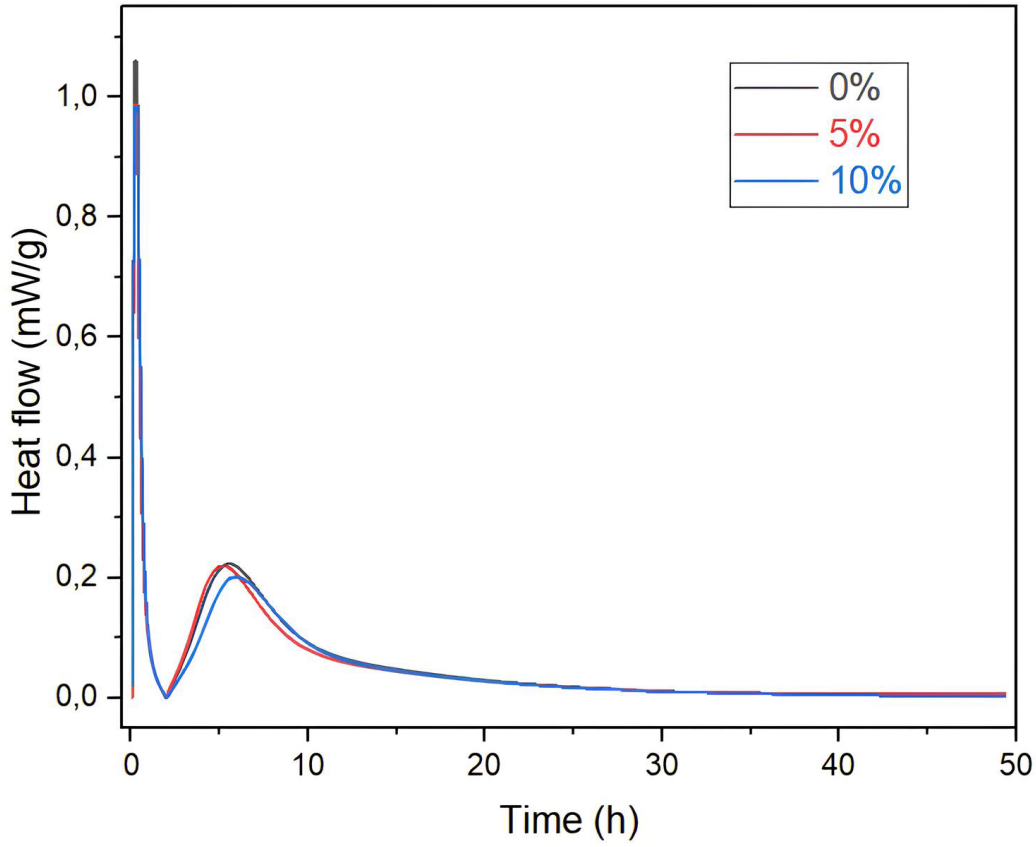

Figure 4. Heat flow of cement pastes with different CA-ash contents (0%, 5% and 10%).

A progressive reduction in the maximum heat flow intensity was observed with increasing CA-ash content, particularly at 10% replacement, indicating lower overall exothermic activity of the system. This behavior is directly related to the non-pozzolanic nature of CA-ash. As a result, the ash does not contribute to secondary hydration reactions, and the reduction in total heat release is governed by the dilution effect, where the partial substitution of cement decreases the clinker fraction available for hydration [38]. Consequently, the exothermic activity is reduced without altering the fundamental hydration mechanism of the system.

Despite this reduction, the general shape of the curves remained consistent across all mixtures, indicating that the presence of CA-ash did not modify the overall hydration mechanism but only affected the kinetic intensity and rate of heat evolution [39]. No significant displacement of the main hydration peak or clear evidence of nucleation acceleration was observed. These findings are consistent with the chemical and mineralogical characteristics discussed in Section 3.1. The predominance of CaO and KCl, combined with the low content of amorphous silica, confirms that CA-ash acts primarily as a filler rather than a reactive component. Therefore, the reduction in heat release is mainly attributed to clinker dilution rather than to changes in hydration chemistry.

This behavior differs from that observed in systems containing metakaolin, where the pozzolanic effect becomes more pronounced at later ages, contributing to the formation of additional C–S–H and increasing hydration products [40]. Similarly, silica enhances hydration due to its high pozzolanic reactivity and its ability to refine the pore structure, leading to a higher hydration degree and improved microstructure [41]. In contrast, fly ash systems typically exhibit a delayed hydration response, with reduced early heat evolution followed by gradual increases at later stages due to slower pozzolanic reactions [42]. For biochar-based systems, both dilution and nucleation effects may occur depending on particle size and composition, although materials derived from lignocellulosic sources tend to behave predominantly as inert fillers [43].

Considering that pastes were tested under controlled calorimetric conditions, while mortars were cured in open laboratory environment, differences in moisture exposure may also contribute to mechanical performance variations.

3.3 Physical and mechanical performance of mortars

The physical and mechanical performance of the mortars was evaluated to investigate how the partial replacement of Portland cement by CA-ash affects both the fresh and hardened states.

The consistency index results are presented in Figure 5. The reference mixture (REF), without ash addition, exhibited a consistency index of 263.65 ± 4.80 mm, demonstrating high workability. With the incorporation of 5% ash (T5), the flow value decreased to 230.55 ± 3.90 mm, while the 10% mixture (T10) further reduced it to 215.40 ± 3.50 mm. Both T5 and T10 values fall below the range established by NBR 13276 [23] for conventional mortar applications, indicating that the reduction in workability is primarily associated with the fine particle size and heterogeneous composition. This effect is related to the increased surface area and non-uniform particle distribution, which raise water demand and internal friction, limiting the mobility of the fresh matrix [44].

These results suggest that CA-ash incorporation influences the rheology primarily through a physical filler effect, increasing internal friction and water demand. This behavior is expected and widely reported for fine particulate materials. Similar trends have been observed for biochar-based systems, where the incorporation of fine carbonaceous particles affects rheology and increases water demand due to their porous structure and surface characteristics [43]. In the case of highly pozzolanic materials such as metakaolin, the reduction in workability is also associated with high specific

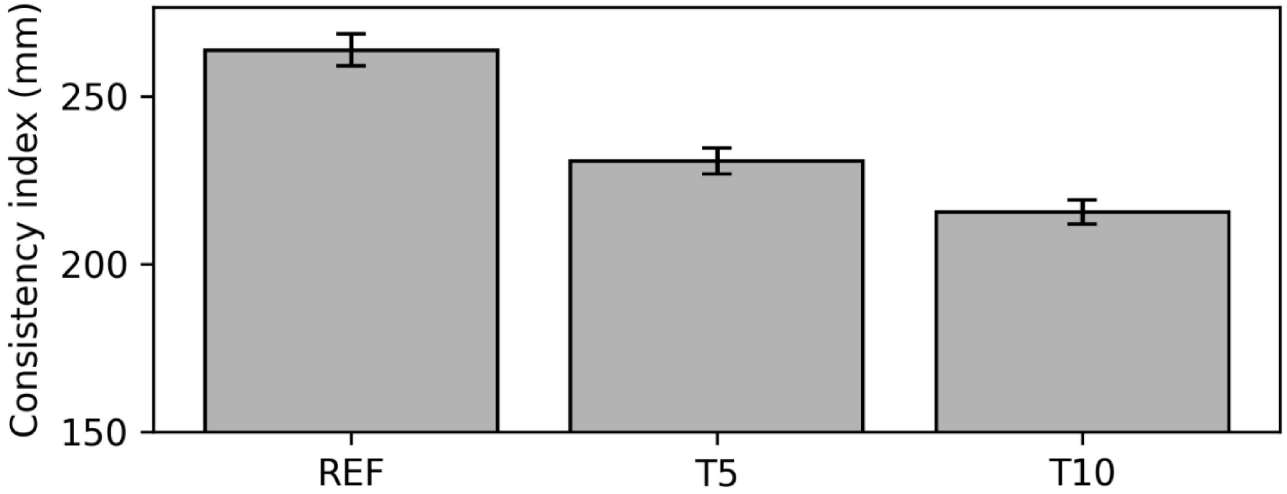

Figure 5. Consistency index of the studied mixtures.

surface area and water adsorption capacity [40]. In contrast, fly ash may improve workability due to its spherical particle morphology and micro-aggregate effect, highlighting that the rheological response depends strongly on particle shape and reactivity [42]. This trend aligns with findings in other studies that examined fine bio-ashes and mineral residues used as partial cement replacements [45].

The compressive strength results at 7 and 28 days are presented in Table 2. At 7 days, REF mixture reached 10.15 ± 0.37 MPa, while T5 achieved 14.54 ± 0.71 MPa and T10 reached 12.37 ± 0.22 MPa. The incorporation of 5% CA-ash resulted in a marked strength increase compared to the reference mixture, whereas the 10% replacement level showed intermediate performance.

At 28 days, the REF mixture reached 10.78 ± 0.58 MPa, while T5 and T10 achieved 14.22 ± 0.89 MPa and 11.45 ± 1.15 MPa, respectively. The 5% mixture maintained the highest compressive strength at both ages.

It is noteworthy that strength development between 7 and 28 days was limited for all mixtures. Although Portland cement systems typically exhibit progressive strength gain over time, the present results showed only minor variations between the evaluated. The statistical evaluation of the curing age factor is presented in Section 3.4. Nevertheless, the limited variation observed between 7 and 28 days already suggests that strength development was not substantially governed by hydration time under the adopted curing conditions.

It is important to consider that the specimens were cured in an open laboratory environment without humidity control. Under these conditions, variations in the effective water-to-binder ratio due to surface drying may have influenced hydration development, particularly at early ages [46,47]. Thus, the observed behavior reflects the combined influence of physical packing, clinker dilution, and environmental curing conditions, limiting additional strength development between 7 and 28 days.

Therefore, the mechanical performance observed reflects primarily the early-age packing effect of CA-ash rather than progressive long-term hydration enhancement. This interpretation is consistent with the calorimetric results presented in Section 3.2, where no evidence of additional reactive contribution from CA-ash was identified.

Although CA-ash was classified as non-pozzolanic, the strength increase observed at 5% replacement is attributed to a physical packing effect, supported by the granulometric compatibility discussed in Section 3.1 [48]. The ash particles likely contributed to improved particle arrangement and reduction of voids within the cementitious matrix. However, at 10% replacement, the dilution effect becomes more pronounced, reducing the effective clinker content available for hydration [49].

The results for water absorption and open porosity at 28 days are presented in Table 3.

The reference mortar recorded 10.66 ± 0.37% for water absorption, while T5 and T10 showed 10.72 ± 0.48% and 10.61 ± 0.17%, respectively. For open porosity, the reference mixture presented 20.25 ± 0.54%, followed by 20.06 ± 0.86% (T5) and 19.54 ± 0.25% (T10).

The differences among mixtures are small and fall within the respective standard deviation ranges, indicating that CA-ash incorporation up to 10% did not significantly modify the pore structure of the mortars [50].

Hence, CA-ash acts mainly as a filler, maintaining matrix compactness and impermeability. The small reduction in the T10 mixture also indicates that the fine ash particles partially filled voids between sand and cement grains, slightly improving microstructural densification [29].

This behavior supports the findings from calorimetry and mineralogical characterization, where the ash was shown to be non-reactive yet physically effective in adjusting the internal packing of solids. Consequently, CA-ash addition up to 10% does not impair the pore structure of mortars.

Regarding apparent density values at 28 days, the results are presented in Figure 6. The reference mortar exhibited 1.89 ± 0.07 g/cm3, while T5 and T10 showed 1.83 ± 0.08 g/cm3 and 1.84 ± 0.07 g/cm3, respectively. The slight decrease with increasing CA-ash content can be associated compared to Portland cement, combined with the absence of additional hydration products capable of densifying the matrix [51]. Even so, the small magnitude of this variation

Table 2. Compressive strength of mortars containing 0%, 5%, and 10% CA-ash at 7 and 28 days

Mixture	7 days (MPa)	28 days (MPa)
REF	10.15 ± 0.37	10.78 ± 0.58
T5	14.54 ± 0.71	14.22 ± 0.89
T10	12.37 ± 0.22	11.45 ± 1.15

Table 3. Water absorption and open porosity of mortars containing 0%, 5%, and 10% CA-ash at 28 days

Mixture	Water absorption (%)	Open porosity index (%)
REF	10.66 ± 0.37	20.25 ± 0.54
T5	10.72 ± 0.48	20.06 ± 0.86
T10	10.61 ± 0.17	19.54 ± 0.25

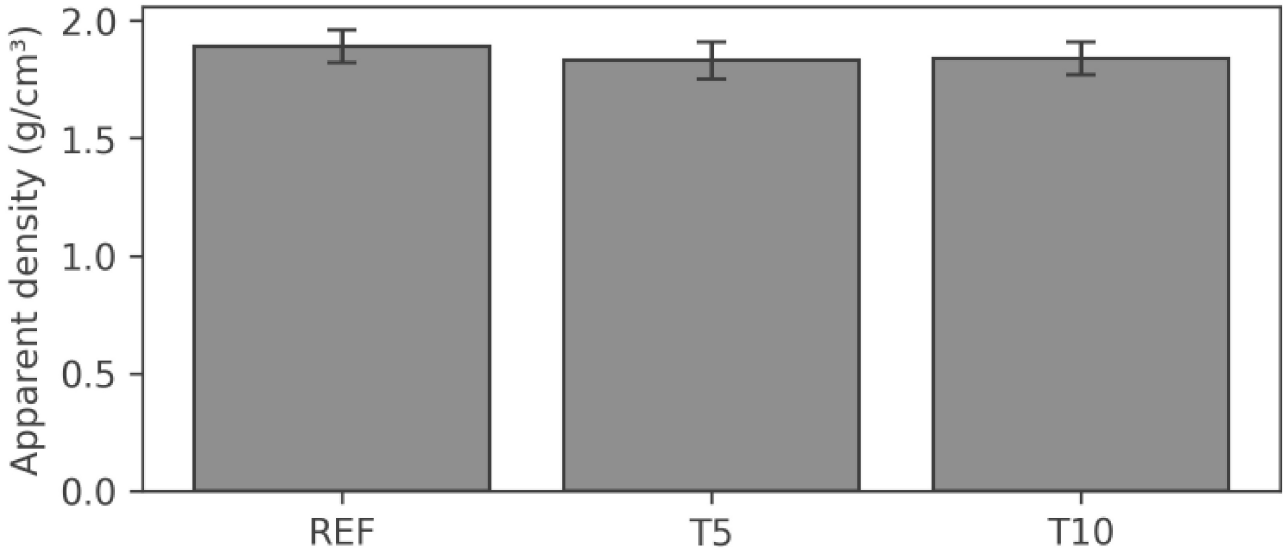

Figure 6. Apparent density of mortars with different CA-ash contents at 28 days.

indicates that the compactness and homogeneity of the mixtures were preserved.

Overall, these density results, combined with stable porosity and absorption data, confirm that CA-ash can be incorporated safely at low levels (< 10%) in non-structural mortars without compromising durability.

3.4 Statistical analysis

In order to verify the statistical significance of the experimental results with respect to the different CA-ash replacement levels, an analysis of variance (ANOVA) was performed for compressive strength, water absorption, open porosity, and apparent density. The significance level adopted was $\alpha = 0.05$.

This statistical approach allows a rigorous evaluation of whether the observed variations among mixtures are associated with material substitution or merely reflect experimental dispersion inherent to cementitious systems [52]. For compressive strength, a two-way ANOVA was conducted considering mixture composition and curing age as independent factors (Table 4).

The results indicate that mixture composition had a highly significant effect on compressive strength ($F = 164.38$; $p = 9.84 \times 10{-}15$), demonstrating that CA-ash replacement level strongly influences mechanical performance. In contrast, curing age did not present statistical significance as an isolated factor ($F = 1.30$; $p = 0.265$), indicating that strength evolution between 7 and 28 days was limited under the studied conditions.

A statistically significant interaction between mixture and age was observed ($F = 6.40$; $p = 0.0059$), confirming that the influence of CA-ash replacement depends on curing time. This interaction reinforces that the 5% replacement level consistently enhances strength, whereas the 10% level reflects the increasing dominance of clinker dilution over packing benefits.

For the physical parameters obtained at 28 days, a two-way ANOVA was performed considering mixture composition and property type (water absorption and open porosity) as independent factors (Table 5).

The statistical analysis demonstrated that mixture composition did not significantly affect the evaluated transport-related properties ($F = 1.90$; $p = 0.172$). Additionally, no significant interaction between mixture and property type was detected ($F = 1.47$; $p = 0.250$), indicating that CA-ash incorporation up to 10% does not statistically modify either water absorption or open porosity.

As expected, the factor "Property" itself was statistically significant ($F = 3376.88$; $p = 2.47 \times 10{-}27$), reflecting the intrinsic numerical difference between water absorption and open porosity values. However, this significance is inherent to the distinct physical definitions of these parameters [53] and does not represent an effect of CA-ash substitution.

For apparent density at 28 days, a one-way ANOVA was conducted considering mixture composition as the independent factor (Table 6). The results revealed a statistically significant effect of mixture composition on apparent density ($F = 17.83$; $p = 0.000254$).

Although the absolute density variations are numerically small, the statistical significance indicates that CA-ash incorporation affects matrix compactness. This behavior is consistent with the physical packing effect suggested by the particle size distribution analysis and the observed mechanical performance trends.

Overall, the statistical results confirm that CA-ash replacement significantly influences compressive strength and apparent density, while water absorption and open porosity remain statistically unaffected within the studied substitution range.

Table 4. Two-way ANOVA results for compressive strength (mixture × age)

Source	F	p-value
Mixture	164.38	< 0.001
Age	1.30	0.265
Mixture x age	6.40	0.0059

Table 5. Two-way ANOVA results for water absorption and open porosity (mixture × property)

Source	F	p-value
Mixture	1.90	0.172
Property	3376.88	< 0.001
Mixture x property	1.47	0.250

Table 6. One-way ANOVA results for apparent density

Source	F	p-value
Mixture	17.83	0.00025

4 Conclusions

This study evaluated the feasibility of using charcoal ash (CA-ash) as a partial replacement for Portland cement in mortars, considering its physicochemical characteristics, hydration behavior, and influence on physical and mechanical properties. Chemical and mineralogical analyses indicated that CA-ash is predominantly composed of CaO (≈69%) and K2O (≈11%), with crystalline phases of quartz and sylvite identified by X-ray diffraction. The Luxán test confirmed the absence of significant pozzolanic activity, indicating that the ash behaves mainly as an inert material.

Particle size analysis revealed a median diameter of approximately 19 μm, comparable to that of Portland cement particles, suggesting that CA-ash may contribute to particle packing through a filler effect. Isothermal calorimetry demonstrated a reduction in heat flow and cumulative heat release with increasing ash content, reflecting the dilution of clinker phases caused by the non-reactive nature of the material.

In the fresh state, CA-ash incorporation reduced mortar workability. The consistency index decreased from 263.65 ± 4.80 mm for the reference mixture to 230.55 ± 3.90 mm and 215.40 ± 3.50 mm for the mixtures containing 5% and 10% ash. This reduction is associated with the fine particle size and heterogeneous composition of the ash, which increases internal friction within the mixture.

Regarding mechanical performance, the mixture containing 5% CA-ash exhibited the highest compressive strength, reaching approximately 14.5 MPa at 7 days, while the reference mixture remained close to 10 MPa. The results indicate that small additions of CA-ash promote a particle packing effect that improves early mechanical performance.

Statistical analysis confirmed that mixture composition significantly affected compressive strength, whereas curing age did not present a statistically significant isolated effect under the studied conditions. Water absorption (≈10.6%) and open porosity (≈20%) did not show statistically significant differences among mixtures, indicating that CA-ash incorporation up to 10% does not significantly alter transport-related properties. Apparent density ranged between 1.83 and 1.89 g/cm3, with statistical analysis indicating a significant influence of mixture composition on this parameter.

The experimental program was conducted under open laboratory curing conditions without strict humidity control, which may have influenced the evolution of compressive strength between testing ages. In addition, the investigation was limited to replacement levels up to 10% and to early curing ages, which restricts broader interpretations of long-term behavior. Even so, the results indicate that CA-ash behaves predominantly as a physical filler, allowing partial replacement of Portland cement while maintaining the compactness and physical stability of the mortar matrix.

Acknowledgements

The authors thank the Carlos Chagas Filho Foundation for Research Support of the State of Rio de Janeiro (FAPERJ), the Coordination for the Improvement of Higher Education Personnel (CAPES), and the National Council for Scientific and Technological Development (CNPq) for the financial support for the preparation of this article.

References

1 Nia SB, Shafei B. Carbon footprint reduction through repurposing solid wastes into sustainable construction materials: a state-of-the-art review. Cleaner and Responsible Consumption. 2025;18:100310. https://doi.org/10.1016/j.clrc.2025.100310.

2 Hossaini N, Hewage K. Sustainable materials selection for Canadian construction industry: an emergy-based life-cycle analysis (Em-LCA) of conventional and LEED suggested construction materials. Journal of Sustainable Development. 2011;5(1). https://doi.org/10.5539/jsd.v5n1p2.

3 Martin L, Perry F. Sustainable construction technology adoption. In: Tam VWY, Le KN, editors. Sustainable construction technologies. Oxford: Butterworth-Heinemann; 2019. p. 299-316. https://doi.org/10.1016/B978-0-12-811749-1.00009-2.

4 Wu T, Ng ST, Chen J. Deciphering the CO2 emissions and emission intensity of cement sector in China through decomposition analysis. Journal of Cleaner Production. 2022;352:131627. https://doi.org/10.1016/j.jclepro.2022.131627.

5 Sabrin R, Shahjalal M, Eema Bachu HA, Lutful Habib MM, Jerin T, Billah AHMM. Recycling of different industrial wastes as supplement of cement for sustainable production of mortar. Journal of Building Engineering. 2024;86:108765. https://doi.org/10.1016/j.jobe.2024.108765.

6 Rocha GJE, Fadini Natalli J, Gonçalves MM, Rangel GAA, Teixeira Marvila M. Use of agroindustrial wastes as pozzolanic materials in cementitious systems: a review. Journal of Materials Research and Technology. 2025;37:4761-4781. https://doi.org/10.1016/j.jmrt.2025.07.031.

7 Oliveira GM, Vitoriano Julio AA, Venturini OJ, Leme MMV, Rezende TTG, Palacio JCE, et al. Energy recovery of gases from charcoal production: potential, available technologies, costs, sustainability, and its contribution to the energy transition in Brazil. Processes. 2026;14(3):511. https://doi.org/10.3390/pr14030511.

8 Mencarelli A, Greco R, Balzan S, Grigolato S, Cavalli R. Charcoal-based products combustion: emission profiles, health exposure, and mitigation strategies. Environmental Advances. 2023;13:100420. https://doi.org/10.1016/j.envadv.2023.100420.

9 Allais F. Barbecue: the chemistry behind cooking on a barbecue. In: Lavelle C, This H, Kelly AL, Burke R, editors. Handbook of molecular gastronomy. 1st ed. Boca Raton: CRC Press; 2021. https://doi.org/10.1201/9780429168703-13.

10 Instituto Brasileiro de Árvores. IBÁ relatório anual 2025. São Paulo: IBÁ; 2025.

11 Liang X, Li Z, Dong H, Ye G. A review on the characteristics of wood biomass fly ash and their influences on the valorization in cementitious materials. Journal of Building Engineering. 2024;97:110927. https://doi.org/10.1016/j.jobe.2024.110927.

12 Souza AE, Teixeira SR, Santos GTA, Costa FB, Longo E. Reuse of sugarcane bagasse ash (SCBA) to produce ceramic materials. Journal of Environmental Management. 2011;92(10):2774-2780. https://doi.org/10.1016/j.jenvman.2011.06.020.

13 Tayeh BA, Alyousef R, Alabduljabbar H, Alaskar A. Recycling of rice husk waste for a sustainable concrete: a critical review. Journal of Cleaner Production. 2021;312:127734. https://doi.org/10.1016/j.jclepro.2021.127734.

14 Suarez-Riera D, Falliano D, Carvajal JF, Celi ACB, Ferro GA, Tulliani JM, et al. The effect of different biochar on the mechanical properties of cement-pastes and mortars. Buildings. 2023;13(12):2900. https://doi.org/10.3390/buildings13122900.

15 Asvesta A, Kapageridis I, Vasileiadou A, Koios K, Kantiranis N. Granulometric, chemical, and mineralogical evaluation of greek lignite bottom ash for potential utilization in concrete manufacturing. Mater. Proc. 2023;15(1):50. https://doi.org/10.3390/materproc2023015050.

16 Associação Brasileira de Normas Técnicas. ABNT NBR 5752: materiais pozolânicos: determinação de índice de desempenho com cimento Portland aos 28 dias. 3. ed. Rio de Janeiro: ABNT; 2014.

17 Associação Brasileira de Normas Técnicas. ABNT NBR 16697: cimento Portland: requisitos. 1. ed. Rio de Janeiro: ABNT; 2018.

18 Associação Brasileira de Normas Técnicas. ABNT NBR 7214: areia normal para ensaio de cimento: especificação. 3. ed. Rio de Janeiro: ABNT; 2015.

19 Snellings R, Almenares Reyes R, Hanein T, Irassar EF, Kanavaris F, Maier M, et al. Paper of RILEM TC 282-CCL: mineralogical characterization methods for clay resources intended for use as supplementary cementitious material. Materials and Structures. 2022;55(5):149. https://doi.org/10.1617/s11527-022-01973-1.

20 Luxán MP, Madruga F, Saavedra J. Rapid evaluation of pozzolanic activity of natural products by conductivity measurement. Cement and Concrete Research. 1989;19(1):63-68. https://doi.org/10.1016/0008-8846(89)90066-5.

21 American Society for Testing and Materials. ASTM 1679-17: standard practice for measuring hydration kinetics of hydraulic cementitious mixtures using isothermal calorimetry. West Conshohocken: ASTM International; 2017. https://doi.org/10.1520/C1679-17.

22 Shahi S, Fakhri E, Yavari H, Maleki Dizaj S, Salatin S, Khezri K. Portland cement: an overview as a root repair material. BioMed Research International. 2022;2022(1):3314912. https://doi.org/10.1155/2022/3314912.

23 Associação Brasileira de Normas Técnicas. ABNT NBR 13276: argamassa para assentamento e revestimento de paredes e tetos: determinação do índice de consistência. Rio de Janeiro: ABNT; 2016.

24 Associação Brasileira de Normas Técnicas. ABNT NBR 7215: cimento Portland: determinação da resistência à compressão de corpos de prova cilíndricos. 2. ed. Rio de Janeiro: ABNT; 2019.

25 Associação Brasileira de Normas Técnicas. ABNT NBR 9778: argamassas e concreto endurecidos: determinação da absorção de água, índice de vazios e massa específica. Rio de Janeiro: ABNT; 2011.

26 Associação Brasileira de Normas Técnicas. ABNT NBR 13280: argamassa para assentamento e revestimento de paredes e tetos: determinação da densidade de massa aparente no estado endurecido. Rio de Janeiro: ABNT; 2005.

27 Sun H, Pang L, Ding Y, Xing B, Tang Y, Sun X, et al. Influence of the physical morphological characteristics of mineral fillers on the bitumen-filler interfacial interaction. Construction & Building Materials. 2023;378:131206. https://doi.org/10.1016/j.conbuildmat.2023.131206.

28 McCarthy MJ, Dyer TD. Pozzolanas and pozzolanic materials. In: Hewlett PC, Liska M, editors. Lea's chemistry of cement and concrete. Oxford: Butterworth-Heinemann; 2019. p. 363-467. https://doi.org/10.1016/B978-0-08-100773-0.00009-5.

29 Begentayev MM, Kuldeyev EI, Akhmetov DA, Zhumadilova ZO, Suleyev DK, Utepov YB, et al. The effect of mineral fillers on the rheological and performance properties of self-compacting concretes in the production of reinforced concrete products. Journal of Composites Science. 2025;9(5):235. https://doi.org/10.3390/jcs9050235.

30 Santos SF, Tonoli GHD, Mejia JEB, Fiorelli J, Savastano H Jr. Non-conventional cement-based composites reinforced with vegetable fibers: a review of strategies to improve durability. Materiales de Construcción. 2015;65(317):e041. https://doi.org/10.3989/mc.2015.05514.

31 Maljaee H, Madadi R, Paiva H, Tarelho L, Ferreira VM. Incorporation of biochar in cementitious materials: A roadmap of biochar selection. Construction & Building Materials. 2021;283:122757. https://doi.org/10.1016/j.conbuildmat.2021.122757.

32 Zhang P, Liao W, Kumar A, Zhang Q, Ma H. Characterization of sugarcane bagasse ash as a potential supplementary cementitious material: comparison with coal combustion fly ash. Journal of Cleaner Production. 2020;277:123834. https://doi.org/10.1016/j.jclepro.2020.123834.

33 Thiedeitz M, Ostermaier B, Kränkel T. Rice husk ash as an additive in mortar: contribution to microstructural, strength and durability performance. Resources, Conservation and Recycling. 2022;184:106389. https://doi.org/10.1016/j.resconrec.2022.106389.

34 Habert G, Choupay N, Montel JM, Guillaume D, Escadeillas G. Effects of the secondary minerals of the natural pozzolans on their pozzolanic activity. Cement and Concrete Research. 2008;38(7):963-975. https://doi.org/10.1016/j.cemconres.2008.02.005.

35 American Society for Testing and Materials. ASTM C618-22: standard specification for coal fly ash and raw or calcined natural pozzolan for use in concrete. West Conshohocken: ASTM International; 2022. https://doi.org/10.1520/C0618-22.

36 Khan MI, Abbas YM, Fares G. Enhancing cementitious concrete durability and mechanical properties through silica fume and micro-quartz. Sustainability. 2023;15(22):15913. https://doi.org/10.3390/su152215913.

37 Walker R, Pavía S. Physical properties and reactivity of pozzolans, and their influence on the properties of lime-pozzolan pastes. Materials and Structures. 2011;44(6):1139-1150. https://doi.org/10.1617/s11527-010-9689-2.

38 Charitha V, Athira VS, Jittin V, Bahurudeen A, Nanthagopalan P. Use of different agro-waste ashes in concrete for effective upcycling of locally available resources. Construction & Building Materials. 2021;285:122851. https://doi.org/10.1016/j.conbuildmat.2021.122851.

39 Smaoui N, Bérubé MA, Fournier B, Bissonnette B, Durand B. Effects of alkali addition on the mechanical properties and durability of concrete. Cement and Concrete Research. 2005;35(2):203-212. https://doi.org/10.1016/j.cemconres.2004.05.007.

40 Jing H, Li M, Zhang Y, Gao M. Hydration kinetics, microstructure and physicochemical performance of metakaolin-blended cementitious composites. Construction & Building Materials. 2023;408:133756. https://doi.org/10.1016/j.conbuildmat.2023.133756.

41 Zhang Z, Zhang B, Yan P. Hydration and microstructures of concrete containing raw or densified silica fume at different curing temperatures. Construction & Building Materials. 2016;121:483-490. https://doi.org/10.1016/j.conbuildmat.2016.06.014.

42 Yu J, Li G, Leung CKY. Hydration and physical characteristics of ultrahigh-volume fly ash-cement systems with low water/binder ratio. Construction & Building Materials. 2018;161:509-518. https://doi.org/10.1016/j.conbuildmat.2017.11.104.

43 Salem T, Fen-Chong T. Clarifying the effect of biochar on the hydration, setting, workability, and mechanical strength of cementitious materials. Construction & Building Materials. 2025;485:141892. https://doi.org/10.1016/j.conbuildmat.2025.141892.

44 Felekoğlu B, Türkel S, Kalyoncu H. Optimization of fineness to maximize the strength activity of high-calcium ground fly ash - Portland cement composites. Construction & Building Materials. 2009;23(5):2053-2061. https://doi.org/10.1016/j.conbuildmat.2008.08.024.

45 Gupta S, Krishnan P, Kashani A, Kua HW. Application of biochar from coconut and wood waste to reduce shrinkage and improve physical properties of silica fume-cement mortar. Construction & Building Materials. 2020;262:120688. https://doi.org/10.1016/j.conbuildmat.2020.120688.

46 Mohan MK, Rahul AV, Villagran-Zaccardi Y, De Schutter G, Van Tittelboom K. A rheometric approach to assess plastic shrinkage and implications of early age drying on the microstructure of cement-based materials. Cement and Concrete Research. 2024;180:107504. https://doi.org/10.1016/j.cemconres.2024.107504.

47 Im S, Liu J, Cho S, Moon J, Park J, Wi K, et al. Quantitative characterization of the interfacial transition zone around lightweight and normal aggregates in cement mortars at different water-to-binder ratios. Construction & Building Materials. 2023;400:132584. https://doi.org/10.1016/j.conbuildmat.2023.132584.

48 Yahia A, Tanimura M, Shimoyama Y. Rheological properties of highly flowable mortar containing limestone filler-effect of powder content and W/C ratio. Cement and Concrete Research. 2005;35(3):532-539. https://doi.org/10.1016/j.cemconres.2004.05.008.

49 Zhao L, Guo X, Song L, Song Y, Dai G, Liu J. An intensive review on the role of graphene oxide in cement-based materials. Construction & Building Materials. 2020;241:117939. https://doi.org/10.1016/j.conbuildmat.2019.117939.

50 Wembe JT, Ngueyep LLM, Elat E, Pliya P, Telefouet AJP, Ndjaka J-MB, et al. Valorization of ashes from different wood species in cementitious materials. Discover Sustainability. 2024;5(1):257. https://doi.org/10.1007/s43621-024-00460-7.

51 Netinger Grubeša I, Šamec D, Juradin S, Hadzima-Nyarko M. Utilizing agro-waste as aggregate in cement composites: a comprehensive review of properties, global trends, and applications. Materials. 2025;18(10):2195. https://doi.org/10.3390/ma18102195.

52 Li Z, Lu D, Gao X. Optimization of mixture proportions by statistical experimental design using response surface method: a review. Journal of Building Engineering. 2021;36:102101. https://doi.org/10.1016/j.jobe.2020.102101.

53 Ren F, Zhou C, Zeng Q, Zhang Z, Angst U, Wang W. Quantifying the anomalous water absorption behavior of cement mortar in view of its physical sensitivity to water. Cement and Concrete Research. 2021;143:106395. https://doi.org/10.1016/j.cemconres.2021.106395.

Received: 24 Oct. 2025
Accepted: 07 May 2026

Editor-in-charge:
André Luiz Vasconcellos da Costa e Silva